

2006

Synthesis of High-Temperature Stable Anatase TiO₂ Photocatalyst

Suresh Pillai

Technological University Dublin, suresh.pillai@tudublin.ie

Declan McCormack

Technological University Dublin, Declan.mccormack@tudublin.ie

Michael Seery

Technological University Dublin, michael.seery@tudublin.ie

See next page for additional authors

Follow this and additional works at: <https://arrow.tudublin.ie/cenresart>

 Part of the [Systems and Communications Commons](#)

Recommended Citation

Pillai, S.C. et al. (2006) Synthesis of High-Temperature Stable Anatase TiO₂ Photocatalyst, *Journal of Physical Chemistry. C*, vol. 111 no. 4, 2007, 1605–1611. doi:10.1021/jp065933h

This Article is brought to you for free and open access by the Crest: Centre for Research in Engineering Surface Technology at ARROW@TU Dublin. It has been accepted for inclusion in Articles by an authorized administrator of ARROW@TU Dublin. For more information, please contact arrow.admin@tudublin.ie, aisling.coyne@tudublin.ie.



This work is licensed under a [Creative Commons Attribution-NonCommercial-Share Alike 4.0 License](#)

Authors

Suresh Pillai, Declan McCormack, Michael Seery, Pradeepan Periyat, Steven Hinder, John Colreavy, Reenamol George, and Hugh Hayden

Synthesis of High-Temperature Stable Anatase TiO₂ Photocatalyst

Suresh C. Pillai,^{*,†} Pradeepan Periyat,^{‡,§} Reenamole George,^{‡,§} Declan E. McCormack,[‡] Michael K. Seery,[‡] Hugh Hayden,[†] John Colreavy,[†] David Corr,[§] and Steven J. Hinder[‡]

Centre for Research in Engineering Surface Technology (CREST), FOCAS Institute, Dublin Institute of Technology, Camden Row, Dublin 8, Ireland, School of Chemical and Pharmaceutical Sciences, Dublin Institute of Technology, Kevin Street, Dublin 8, Ireland, Ntera Ltd., 58 Spruce Avenue, Stillorgan Industrial Park, Blackrock, Co., Dublin, Ireland, and The Surface Analysis Laboratory, School of Engineering, University of Surrey, Guildford, Surrey, GU2 7XH, United Kingdom

Received: September 12, 2006; In Final Form: November 9, 2006

In the absence of a dopant or precursor modification, anatase to rutile transformation in synthetic TiO₂ usually occurs at a temperature of 600–700 °C. Conventionally, metal oxide dopants (e.g., Al₂O₃ and SiO₂) are used to tune the anatase to rutile transformation. A simple methodology is reported here to extend the anatase to rutile transformation by employing various concentrations of urea. XRD and Raman spectroscopy were used to characterize various phases formed during thermal treatment. A significantly higher anatase phase (97%) has been obtained at 800 °C with use of a 1:1 Ti(OPr)₄:urea composition and 11% anatase composition is retained even after calcining the powder at 900 °C. On comparison a sample that has been prepared without urea showed that rutile phases started to form at a temperature as low as 600 °C. The effect of smaller amounts of urea such as 1:0.25 and 1:0.5 Ti(OPr)₄:urea has also been studied and compared. The investigation concluded that the stoichiometric modification by urea 1:1 Ti(OPr)₄:urea composition is most effective in extending the anatase to rutile phase transformation by 200 °C compared to the unmodified sample. In addition, BET analysis carried out on samples calcined at 500 °C showed that the addition of urea up to 1:1 Ti(OPr)₄:urea increased the total pore volume (from 0.108 to 0.224 cm³/g) and average pore diameter (11 to 30 nm) compared to the standard sample. Samples prepared with 1:1 Ti(OPr)₄:urea composition calcined at 900 °C show significantly higher photocatalytic activity compared to the standard sample prepared under similar conditions. Kinetic analysis shows a marked increase in the photocatalytic degradation of rhodamine 6G on going from the standard sample (0.27 min⁻¹, decoloration in 120 min) to the urea-modified sample (0.73 min⁻¹, decoloration in 50 min).

1. Introduction

Nanocrystalline titania (TiO₂) has received significant attention in the last few decades due to the photoinduced electron-transfer properties associated with the anatase metastable phase.^{1–3} Titania usually exists in three different forms: anatase (tetragonal, $a = b = 3.78 \text{ \AA}$; $c = 9.50 \text{ \AA}$), rutile (tetragonal, $a = b = 4.58 \text{ \AA}$; $c = 2.95 \text{ \AA}$), and brookite (rhombohedral, $a = 5.43 \text{ \AA}$; $b = 9.16 \text{ \AA}$; $c = 5.13 \text{ \AA}$). These crystalline structures consist of [TiO₆]²⁻ octahedra, which share edges and corners in different manners while keeping the overall stoichiometry as TiO₂.^{4–7} Even though anatase has more edge sharing octahedra, the interstitial spaces between octahedra are larger, which makes rutile denser than anatase (the density of anatase is 3.84 g/cm³ and that of rutile is 4.26 g/cm³).^{4–7} Among the various phases of titania reported, anatase shows a better photocatalytic activity and antibacterial performance.^{8–12} A stable anatase phase up to the sintering temperature of the ceramic substrates is most desirable for applications on antibacterial self-cleaning building materials (e.g., bathroom tile, sanitary ware, etc.).^{13–15} These applications require high-purity

titania with a definite phase composition.^{13–15} The production of high-photoactivity material with high-temperature anatase phase stability is one of the key challenges in smart coating technology. Anatase-to-rutile transformation in pure titania usually occurs at 600 to 700 °C.^{16–18} Phase transition to rutile is nonreversible due to the greater thermodynamic stability of rutile phase.^{19–20} Researchers at Toto Ltd. recently reported²¹ a method to produce photoactive titania-Ag coatings on ceramic materials. The composition contains up to 7% anatase present at 900 °C.²¹ Any improvement in the anatase phase composition at these high temperatures is expected to show a higher photocatalytic activity.²¹ Conventionally metal oxide doping is used to extend the anatase-to-rutile transformation temperature above 700 °C.^{22–26} Various metal oxide dopants such as Al₂O₃, NiO, SiO₂, ZrO₂, ZnO, and Sb₂O₅ have already been studied to assess the effect on both anatase-to-rutile transformation and alteration of modification on textural properties of titania.^{22–26} Formation of secondary impurity phases (e.g., Al₂TiO₅, NiTiO₃) at high temperature is the main disadvantages of this technique. Modifying the precursor characteristics by employing chelating agents is another approach attempted earlier to obtain titania having specific properties.^{27–28} Recent research showed that urea has little effect on the phase formation in titania.²⁹ Previously, urea has been employed to improve the pore parameters and morphology by utilizing it as a pore-forming agent.^{29–31} Zheng et al. reported preparation of mesoporous titania via sol-gel

* Address correspondence to this author. E-mail: suresh.pillai@dit.ie.

† FOCAS Institute, Dublin Institute of Technology.

‡ School of Chemical and Pharmaceutical Sciences, Dublin Institute of Technology.

§ Ntera Ltd.

[‡] School of Engineering, University of Surrey.

74 reactions by using urea as a template.³² Bakardjieva et al.
 75 showed the formation of TiO₂ nanocrystals from titanoyloxy
 76 chloride by using urea as a precipitating agent.³³ Also there are
 77 recent reports published which explain the visible light activity
 78 of titania by doping with nitrogen where urea or thiourea is
 79 used as a precursor.^{34–37} However, there is no systematic study
 80 available in the literature on the effect of various concentrations
 81 of urea on high-temperature stability of anatase. Here in our
 82 study the titania precursor gel has been prepared by hydrolysis
 83 and condensation reaction of titanium isopropoxide (Ti(OPr)₄)
 84 with various mole ratios of urea. The phase transformation
 85 during heat treatment was investigated by X-ray powder
 86 diffraction (XRD). The current study showed that a major
 87 anatase phase (up to 97%) can be retained at 800 °C by
 88 modifying titanium isopropoxide with urea. On the other hand,
 89 the standard titania showed the presence of rutile at a temper-
 90 ature as low as 600 °C. This method has therefore been found
 91 to be effective in extending the anatase-to-rutile phase trans-
 92 formation by at least 200 °C without using any metal oxide
 93 additives. Titania composition prepared by 1:1 Ti(OPr)₄:urea
 94 molar ratio calcined at 900 °C shows significantly higher
 95 photocatalytic activity compared to the standard sample. Deg-
 96 radation kinetics on a model dye, rhodamine 6G, demonstrate
 97 that the urea-modified sample is more than three times as
 98 efficient as the standard sample, a fact attributed to the increased
 99 amount of anatase in the urea-modified sample.

100 2. Experimental Methods

101 The reagents used in this study were titanium isopropoxide
 102 (Aldrich) and urea (Aldrich). In a typical experiment to
 103 synthesize 1:1 titania precursor:urea solution, 46.80 mL of
 104 titanium isopropoxide (Ti(OPr)₄) was added into 412 mL of
 105 isopropanol. To the above solution, 10 g of urea dissolved in
 106 70 mL of water was added. The solution was then stirred for 5
 107 min and aged for 2 h at room temperature. It was then dried at
 108 80 °C for 24 h. The dried powder was calcined at a constant
 109 heating rate of 5 deg/min at 500, 600, 700, 800, 900, and 1000
 110 °C and held at these temperatures for 2 h.

111 The same procedure is adopted to synthesize 1:0.25 and 1:0.5
 112 Ti(OPr)₄:urea samples. A standard sample without urea was also
 113 prepared to compare the results. XRD patterns of the calcined
 114 gels were obtained with a Siemens D 500 X-ray diffractometer
 115 in the diffraction angle range 2θ = 20–70°, using Cu Kα
 116 radiation. The amount of anatase in the sample was estimated
 117 by using the Spurr equation (eq 1)³⁸

$$F_A = 100 - \left(\frac{1}{1 + 0.8(I_A(101)/I_R(110))} \right) 100 \quad (1)$$

118 where F_A is the mass fraction of anatase in the sample and I_A -
 119 (101) and I_R (110) are the integrated main peak intensities of
 120 anatase and rutile, respectively.

121 The BET (Brunauer, Emmett, and Teller) surface area
 122 measurements and pore analysis were carried out by nitrogen
 123 adsorption with use of a Micromeritics Gemini 2375 surface
 124 area analyzer. The measurements were carried out at liquid
 125 nitrogen temperature after degassing the powder samples for 1
 126 h 30 min at 200 °C.

127 Differential Scanning Calorimetry (DSC) measurements were
 128 carried out with a Rheometric Scientific DSC QC. A small
 129 amount of the dried sample (less than 3 mg) was heated from
 130 room temperature (25 °C) to 400 °C at a constant heating rate
 131 of 10 deg/min.

The FTIR spectra of the gel dried at 80 °C was measured by
 using a Spectrum GX-FTIR spectrophotometer in the wave
 number range 4000–400 cm⁻¹, using 70 scans per sample.

X-ray Photoelectron Spectroscopy (XPS) analyses were
 performed on a Thermo VG Scientific (East Grinstead, UK)
 Sigma Probe spectrometer. The instrument employs a mono-
 chromated Al Kα X-ray source ($h\nu = 1486.6$ eV), which was
 used at 140 W. The area of analysis was approximately 500
 μm diameter for the samples analyzed. For survey spectra a
 pass energy of 100 eV and a 0.4 eV step size were employed.
 For C_{1s} and Ti_{2p} high-resolution spectra a pass energy of 20 eV
 and a 0.1 eV step size were used. For O_{1s} high-resolution spectra
 a pass energy of 20 eV and a 0.2 eV step size were used. For
 N_{1s} high-resolution spectra a pass energy of 50 eV and a step
 size of 0.2 eV were used. Charge compensation was achieved
 by using a low-energy electron flood gun. Quantitative surface
 chemical analyses were calculated from the high-resolution core
 level spectra, following the removal of a nonlinear Shirley
 background. The manufacturer's Avantage software was used,
 which incorporates the appropriate sensitivity factors and
 corrects for the electron energy analyzer transmission function.

Photocatalysis Studies. In a typical experiment, a 0.06 g
 standard sample calcined at 900 °C was dispersed in 50 mL of
 Rhodamine 6G solutions having a concentration of 5×10^{-6}
 M. The above suspension was irradiated in a Q-Sun Xenon solar
 simulator chamber (0.68 W/m² at 340 nm) with stirring.
 Degradation was monitored by taking aliquots at increasing time
 intervals. These aliquots were centrifuged and absorption spectra
 of the samples were recorded. Similar experiments were carried
 out for urea modified sample calcined at 900 °C. The rate of
 degradation was assumed to obey pseudo-first-order kinetics
 and hence the rate constant for degradation, k , was obtained
 from the first-order plot according to eq 2

$$\ln\left(\frac{A_0}{A}\right) = kt \quad (2)$$

where A_0 is the initial absorbance, A is the absorbance after a
 time (t) of the rhodamine dye degradation, and k is the first-
 order rate constant.

168 3. Results

3.1. FTIR Spectroscopy. FTIR spectra of the precursor
 samples dried at 80 °C have been recorded. The absorption band
 at 3500–3000 and 1600 cm⁻¹ in all spectra indicate hydroxyl
 group stretching vibrations.²⁹ The broad peak at 500 cm⁻¹ found
 in the standard and urea modified samples indicates the Ti–
 O–Ti stretching vibrations.²⁹ The peak observed at 1035 cm⁻¹
 corresponds to the Ti–O–C bond. The Ti–O–C bond is
 predicted to be the result of the interaction between the Ti–O
 network and the C=O in the urea.²⁹ The peaks corresponding
 to Ti–O–C bond increase in intensity when the urea concentra-
 tion increases (Supporting Information Figure 1). This is a good
 indication that there is a great degree of interaction between
 the inorganic and organic components by the condensation
 reaction. The peak obtained at 1154 cm⁻¹ is assigned to the
 stretching vibration of C–N.²⁹ The peak obtained at 1453 cm⁻¹
 is due to the deformation mode of ammonium ions formed by
 the decomposition of excess urea.⁴⁰ FTIR results thus show a
 strong chelation of urea molecules to the titania precursor. It
 has been observed that the peaks at 1035 (which is assigned
 for the Ti–O–C bond) and 1154 cm⁻¹ (C–N) were absent
 above a calcination temperature of 200 °C and all additional
 peaks except Ti–O stretching are absent above 300 °C.

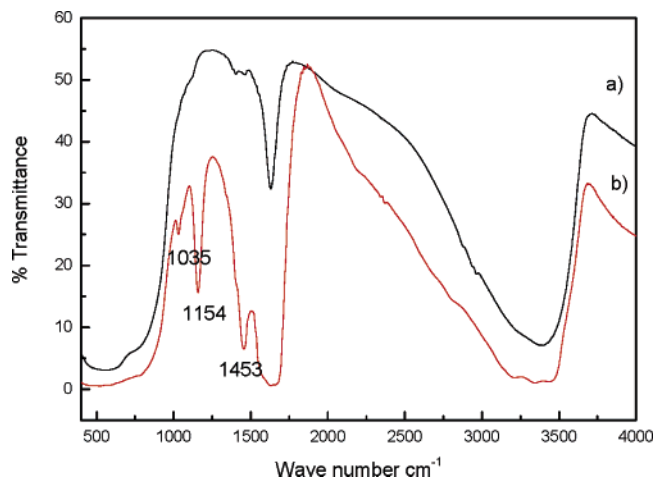


Figure 1. FTIR spectra of the 80 °C dried titania precursor: (a) standard sample and (b) sample of 1:1 Ti(OPr)₄:urea composition.

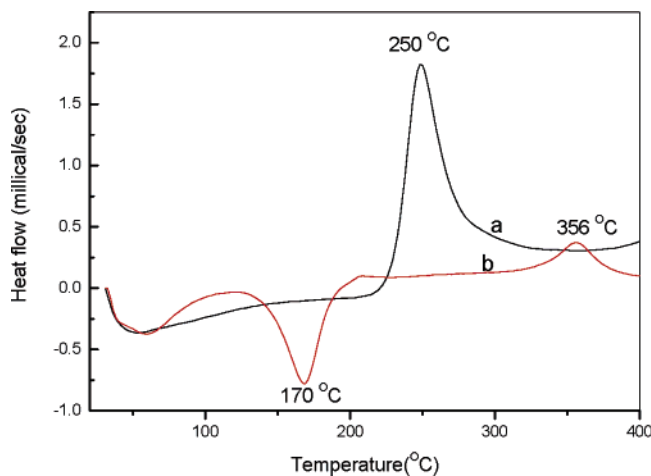


Figure 2. Differential scanning calorimetry of (a) standard and (b) sample of 1:1 Ti(OPr)₄:urea composition.

TABLE 1: BET Surface Area Analysis at 500 °C

material	surface area (m ² /g)	total pore vol (cm ³ /g)	av pore diameter (nm) ±10%
standard TiO ₂ sample	38	0.108	11
1:1 Ti(OPr) ₄ :urea composition	30	0.224	30

3.2. Differential Scanning Calorimetry (DSC). Differential Scanning Calorimetry (DSC) studies have been carried out (Figure 2) to investigate the amorphous-to-crystalline transition of the titania precursor. An endothermic peak at 170 °C has been observed for the 1:1 Ti(OPr)₄:urea sample and this peak has been assigned as the thermal decomposition of the titania–urea precursor. The exothermic peaks (Figure 2a,b) at 250 and 356 °C respectively for the standard and 1:1 Ti(OPr)₄:urea samples indicate the amorphous-to-crystalline formation.²⁷ It is therefore evident from Figure 2 that the amorphous-to-crystalline formation is delayed in the case of the urea-modified sample. XRD analysis has been conducted to confirm the crystallization characteristics at 250 °C. An amorphous phase was obtained for the 1:1 Ti(OPr)₄:urea samples while a crystalline anatase phase was observed for the standard sample (Supporting Information Figure 2).

3.3. Surface Area Measurements. BET surface area and total pore volume are calculated at $p/p_0 = 0.99$ by the BET method

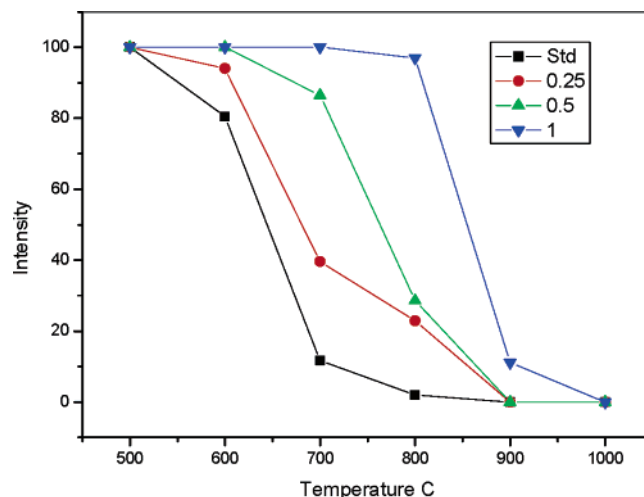


Figure 3. Anatase content in the samples calcined at various temperatures.

for the samples calcined at 500 °C. The results are shown in Table 1. Both isotherms for the standard and urea added samples are type IV-like in their behavior (Supporting Information Figure 3). An earlier report³² shows that the urea is a good pore forming agent so that it will help in the generation of mesoporosity in the titania framework. The current study also confirms that the addition of urea (1:1) increases the pore diameter to 30 nm compared to the 11 nm pore diameter of the standard sample (Table 1). BET analysis of the samples calcined at higher temperatures showed that the 1:1 Ti(OPr)₄:urea sample possesses a higher surface area (15 m²/g) at 800 °C compared to the standard sample calcined (5 m²/g) at the same temperature. The surface area of both the 1:1 Ti(OPr)₄:urea sample and the standard sample at 900 °C showed surface areas of 5 and 4 m²/g, respectively.

3.4. XRD Analysis. Titania precursor samples prepared with urea indicated a significant rise in transformation temperature of anatase to rutile. As the amount of urea increased, the transformation temperature is also raised to higher temperatures (Figure 3).

The weight fraction of the anatase found in the sample was calculated by comparing the XRD integrated intensities of (101) reflection of anatase and (110) reflection of rutile. All the samples heated to 500 °C show only anatase phase (Figure 3). The standard sample showed the formation of rutile at a temperature as low as 600 °C (the anatase content was calculated as 80%). However, all the urea-modified samples except the 1:0.25 (only 6% rutile; 94% anatase) calcined at 600 °C show a complete anatase phase, indicating that a lower percentage of urea has little effect on the anatase rutile transformation (Supporting Information Figure 4).

At 700 °C the standard sample showed rutile as the major phase with 12% anatase (Figure 3) while the samples with 1:0.25 and 1:0.5 Ti(OPr)₄:urea composition showed the presence of 40% and 86% anatase, respectively (Supporting Information Figure 5). At 800 °C standard (Figures 3 and 4, and Supporting Information Figure 6), 1:0.25 and 1:0.5 Ti(OPr)₄:urea composition showed a lower anatase content (0%, 23%, and 27%, respectively). A significantly high anatase content (97%) was obtained for sample with the highest urea content, i.e., 1:1 Ti(OPr)₄:urea, up to a temperature of 800 °C (Figures 3 and 4). All the samples except a sample with the composition of 1:1 Ti(OPr)₄:urea turned to fully rutile at 900 °C. The sample with

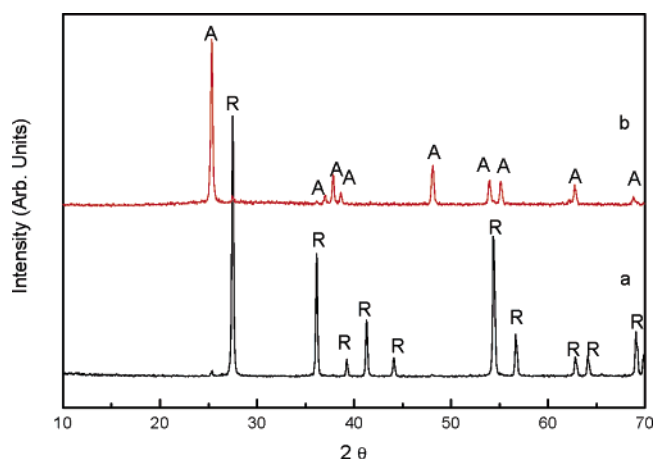


Figure 4. XRD of the samples calcined at 800 °C (A = anatase; R = rutile) of (a) standard sample and (b) sample prepared by 1:1 Ti(OPr)₄:urea composition.

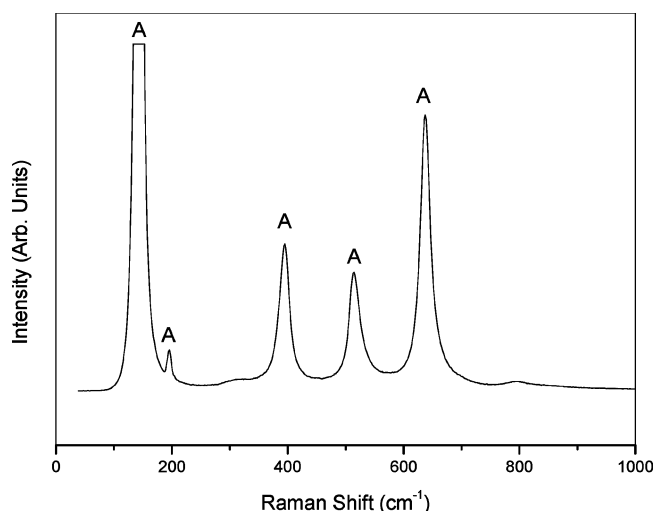


Figure 5. Raman spectra of titania sample with 1:1 Ti(OPr)₄:urea calcined at 800 °C (A = anatase).

a composition of 1:1 Ti(OPr)₄:urea showed 11% anatase at 900 °C (Supporting Information Figure 7).

XRD studies concluded that the modification by urea 1:1 Ti(OPr)₄:urea has been effective in increasing the anatase-to-rutile transformation to high temperature.

3.5. Raman Studies. Raman spectroscopy was applied as an additional tool to probe the phase formation of standard (Supporting Information Figures 8 and 9) and 1:1 Ti(OPr)₄:urea titania samples. Figures 5 and 6 show Raman spectra obtained with samples of composition 1:1 Ti(OPr)₄:urea calcined at 800 and 900 °C. According to factor group analysis the anatase phase consists of six and the rutile phase consists of five Raman active modes (i.e., anatase—144, 197, 399, 513, and 639 cm⁻¹; rutile—144, 446, 612, and 827 cm⁻¹). Figure 5 shows a strong peak at 197 cm⁻¹, which is the characteristic peak of the anatase phase. The peak at 197 cm⁻¹ appears along with other characteristic rutile phases in Figure 6 indicating the presence of the anatase phase in the 900 °C calcined sample. These two Raman spectra are consistent with the XRD results.

3.6. X-ray Photoelectron Spectroscopy (XPS). XPS measurements have been carried out to determine N or C incorporation above 500 °C (Figure 7; Supporting Information Figure 10). The presence of C (ca. 11%) and N (ca. 0.5%) was confirmed in the XPS analysis (Table 2). It was previously reported that the N_{1s} peak will show a binding energy value of

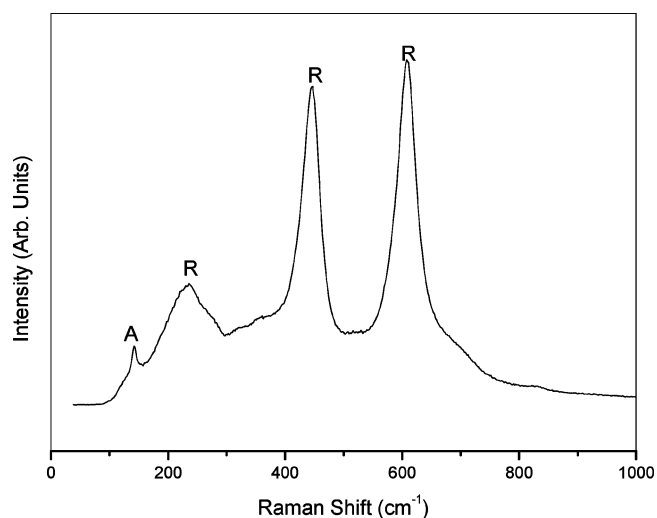


Figure 6. Raman spectra of titania sample with 1:1 Ti(OPr)₄:urea calcined at 900 °C (A = anatase; R = rutile).

400–402 eV and C_{1s} will show a binding energy of 281–287 eV.⁴¹ The signal (Figure 7a) observed at 400 eV was explained previously as a result of the molecular chemisorbed nitrogen.^{42,43} However, there was no indication of Ti–N bond formation (396 eV).⁴²

Three forms of carbon have been identified previously which are surface adsorbed (287.5 eV), solid solution (285 eV), and the carbide Ti–C (281.5 eV).⁴¹ It can be seen from the XPS spectra (Figure 7b) of C_{1s} that the majority of the carbon present in the TiO₂ matrix exists as a solid solution (285 eV). A small surface adsorbed carbon peak is found in all the samples even though the intensity of this peak decreases at 800 °C. There is no indication of the formation of any Ti–C phase. Carbon can locate as a solid solution within the tetrahedral and octahedral interstices existing within the anatase crystal.⁴¹

3.7. Photocatalytic Studies. Photocatalytic studies have been carried out by studying the decomposition reaction of rhodamine dye in the presence of standard and the urea modified samples. The urea modified sample 1:1 Ti(OPr)₄:urea shows more than three times the activity of the unmodified titania. The full decolorization of the rhodamine dye occurred within 50 min in the case of 1:1 Ti(OPr)₄:urea sample calcined at 900 °C whereas the standard sample takes more than 120 min to complete the degradation process. This enhanced efficiency is reflected in a kinetic analysis of the results. The degradation process, involving hydroxyl radical formation and subsequent degradation of the dye by the hydroxyl radical, obeys pseudo-first-order kinetics. First-order degradation rate constants, obtained by plotting the natural logarithm of the absorbance against irradiation time, are $0.27 \pm 0.02 \text{ min}^{-1}$ for the standard sample and $0.73 \pm 0.06 \text{ min}^{-1}$ for the urea-modified sample. A similar trend is observed with the urea-modified sample calcined at 800 °C, which has more than three times the degradation rate of the standard (Supporting Information Figure 11). An initial lag is also observed with this sample. This lag time was about 10 min for both samples and may be due to a slower adsorption of the dye onto the urea-modified sample. Dark studies, where the above experiments were repeated in the absence of a light source, were studied to eliminate any adsorption effects on the studies. Sample left for up to 24 h showed little change in absorbance. The kinetic plots and the progress of the reactions are shown in Figure 8.

The calcination temperature of the sample affects the catalytic efficiency. Both standard and urea modified samples were

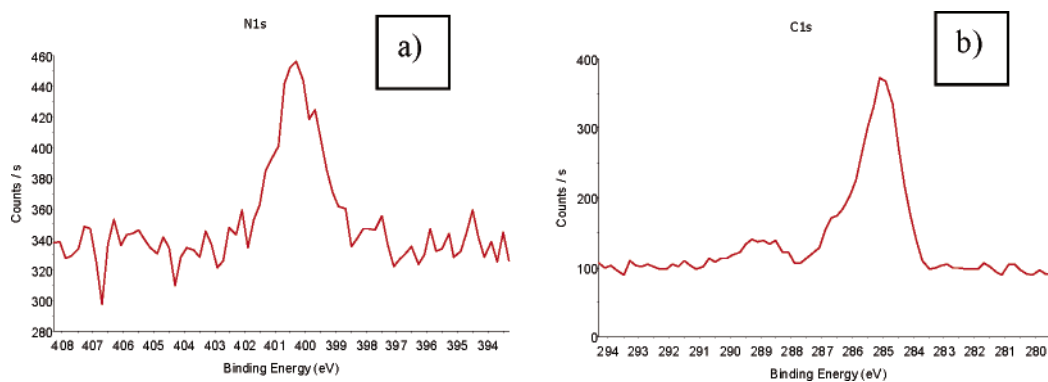


Figure 7. XPS plots of 1:1 Ti(OPr)₄:urea sample calcined at 800 °C: (a) N_{1s} and (b) C_{1s}.

TABLE 2: XPS Analysis of the 1:1 Ti(OPr)₄:Urea Sample Calcined in the Range 500–800 °C

O ₂ sample	Ti	C _{1s} /at %	O1s/at %	Ti2p/At %	N1s/at %
S1	500 °C	12.2	63.0	24.4	0.4
S2	600 °C	12.5	63.2	23.9	0.5
S3	700 °C	11.3	63.8	24.4	0.5
S4	800 °C	11.1	64.0	24.3	0.5

321 calcined at 500, 600, 700, 800, and 900 °C. For the standard
 322 samples, the most efficient photocatalyst was found to be the
 323 sample calcined at 600 °C, whereas for the urea-modified sample
 324 the most efficient temperature was found to be 900 °C
 325 (Supporting Information Figure 12 and Table 1).

326 4. Discussion

327 Titanium tetraisopropoxide hydrolyzes vigorously with water
 328 and polycondensates of [Ti(OH)_nX_m]^{z-} ions are initially formed.
 329 (When the alkoxide reacts with water the metal ion increases
 330 its coordination by employing its vacant d-orbitals to accept
 331 oxygen lone pairs from ligands such as OH groups.) The linkage
 332 between TiO₆²⁻ octahedron is formed by the dehydration
 333 reaction of [Ti(OH)_nX_m]^{z-}. It was previously reported that the
 334 anatase phase has an edge-shared TiO₆²⁻ octahedra structure
 335 while rutile has a corner-shared octahedra.⁴ The condensation
 336 reaction can also be catalyzed in acidic or basic conditions to
 337 make TiO₆²⁻ octahedral from [Ti(OH)_nX_m]^{z-}. Urea is used here
 338 to modify the condensation reaction since gel modifiers are
 339 known to control the pore characteristics.²⁷ The current investigation
 340 also showed that a modifier, urea, can extend the anatase

341 formation to higher temperatures without using any metal or
 342 metal oxide dopants. It was previously proved that the precursor
 343 processing conditions could influence significantly the high-
 344 temperature properties of various nanocrystalline metal oxides
 345 such as ZnO.^{44–46} It should also be noted that the high-
 346 temperature anatase phase stability has been achieved previously
 347 by using copper sulfate as a dopant precursor.⁴⁷ However, when
 348 a precursor without any metal ions (1:1 Ti(OPr)₄:H₂SO₄) was
 349 used a major rutile phase was (63%) formed at 800 °C
 350 (Supporting Information Figure 12).

351 One of the major problems in the preparation of nanocrystalline
 352 TiO₂ is the fast reactivity of inorganic precursor toward
 353 hydrolysis and condensation.^{48–50} Urea molecules chelated to
 354 the Ti ions have amino groups with a high electronegativity
 355 which retard the condensation reactions of titanium isopropoxide
 356 by altering the reaction pathway.²⁹ The chelation is evidenced
 357 from FTIR data which show a strong peak at 1035 cm⁻¹
 358 corresponding to the Ti–O–C bond formed by the interaction
 359 between the Ti–O inorganic network and the C=O of urea
 360 (Figure 1). As the urea content is increased the chelation
 361 becomes stronger and this facilitates a stronger titania gel
 362 network. This is clearly seen from the FTIR results where the
 363 band at 1035 cm⁻¹ is weaker at lower urea concentration and
 364 increases in intensity with an increase in urea concentration. It
 365 has been previously reported that a gel network with little
 366 branching and cross linking with a smaller void region is
 367 morphologically weak and collapses easily on calcinations.³⁹
 368 Therefore strengthening the gel network with urea assists the
 369 retention of the anatase phase to higher temperatures. Further-
 370 more, the uniform distribution of titania precursor molecules
 371 in a urea-stabilized gel network is considered to have caused
 372 the reduction in the anatase/anatase contact points that possibly
 373 reduces the growth process of anatase particles, and this
 374 subsequently promotes pore growth.¹⁸ Therefore the onset of
 375 the nucleation process associated with rutile formation is
 376 delayed.

377 The efficiency of electron–hole formation in a photocatalytic
 378 reaction is dependent on the band gap and the frequency of
 379 incident light, and how competitive electron–hole recombination
 380 is with the parallel electron–oxygen and hole–water reactions.^{51–53}
 381 The anatase phase is found to be a better photocatalyst than
 382 rutile in spite of the fact that the band gap of rutile (3.0 eV) is
 383 smaller than that of anatase (3.2 eV). A faster electron–hole
 384 recombination is feasible in rutile as the recombination prob-
 385 ability is inversely proportional to the magnitude of the band
 386 gap.⁵² It has also been reported that a mixture of anatase and
 387 rutile is more photoactive than 100% anatase.^{51,52} The com-
 388 mercial photocatalyst Degussa P-25 consisting of an anatase/
 389 rutile proportion of 70/30 is more active than pure anatase or
 390 pure rutile.⁵¹ Various preparation methods of the sample which

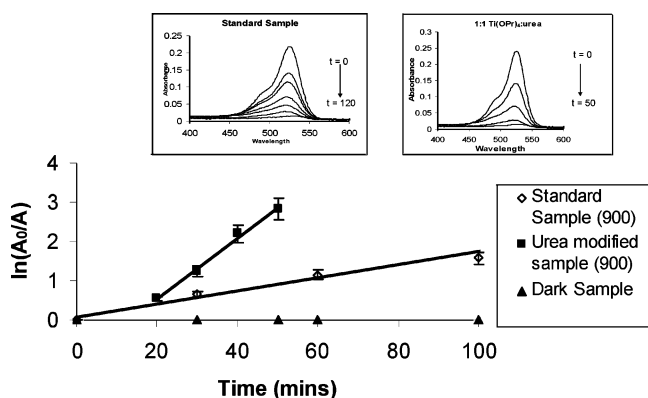


Figure 8. Kinetic study of standard sample and 1:1 Ti(OPr)₄:urea calcined sample at 900 °C. A₀ is the initial absorbance and A is the absorbance after a time of the rhodamine dye degradation. (Error bars ±10%.) The best fit for the urea-modified sample is shown excluding the lag time. Inset: Absorption spectra of rhodamine dye degradation, using standard sample (left inset) and sample with 1:1 Ti(OPr)₄:urea (right inset).

391 result in different crystal structures or surface morphologies were
 392 also found to produce different recombination lifetimes and
 393 interfacial electron-transfer rate constants.^{53–55} It has been
 394 observed in the current study that an anatase/rutile proportion of
 395 11/89 required less than half of the time to degrade rhodamine
 396 dye compared to the 100% rutile sample. The larger amount of
 397 the anatase phase is the most likely cause for higher activity of
 398 the urea-modified sample toward the degradation of the
 399 rhodamine dye.

400 5. Conclusions

401 A method for making the high-temperature stable anatase
 402 phase without using any complex dopants has been reported.
 403 Ninety-seven percent anatase phase has been obtained at 800
 404 °C with use of a 1:1 Ti(OPr)₄:urea composition and 11% of
 405 anatase is retained even after calcining at 900 °C. The current
 406 technique is, therefore, found to be effective in extending the
 407 anatase-to-rutile phase transformation by at least 200 °C
 408 compared to the standard samples. A significantly higher
 409 photoactivity has been achieved for sample modified using urea,
 410 calcined at 900 °C compared to the sample prepared without
 411 using urea calcined under similar conditions. Kinetic analysis
 412 shows that for the urea-modified sample at 900 °C, the
 413 decomposition rate of rhodamine 6G is almost three times faster
 414 due to the presence of the anatase phase at this temperature.
 415 This methodology is therefore suitable for the high-temperature
 416 photocatalytic application in building materials (e.g., ceramics,
 417 glass, and bricks).²¹ A high-temperature stable anatase phase,
 418 good photocatalytic activity, and simplicity of processing are
 419 the main advantages of this method. The characterization of
 420 the materials has been supported by XRD, XPS, DSC, Raman,
 421 FTIR, and surface area analysis. The investigation confirmed
 422 the use of urea as a potential candidate, both as a pore-forming
 423 agent to create mesoporosity in titania and also to obtain the
 424 high-temperature stabilized anatase phase. This approach is very
 425 effective and significant to a considerable extent in dispensing
 426 with the conventional use of metal oxide dopants to retain the
 427 anatase phase at high temperatures. The transformation tem-
 428 perature is expected to increase at a much higher temperature
 429 with the simultaneous use of precursor modification and metal
 430 oxide dopant addition. More studies are underway in this
 431 direction.

432 **Acknowledgment.** This work has been carried out as part
 433 of the innovation partnership between NTERA Ltd. and Dublin
 434 Institute of Technology. The authors gratefully acknowledge
 435 the financial support of Enterprise Ireland and NTERA Ltd.,
 436 Dublin, Ireland. P.P. and R.G. thank R&D Strand I award 2005.
 437 The authors thank Dr. Anthony Betts for his valuable comments.

438 **Supporting Information Available:** Tables five BET
 439 surface area analysis and XPS analysis of Ti(OPr)₄:urea and
 440 figures giving FTIR spectra, Raman spectra, XPS plots and
 441 XRD. This material is available free of charge via the Internet
 442 at <http://pubs.acs.org>.

443 References and Notes

444 (1) Gratzel, M. *Nature* **2001**, *414*, 338.
 445 (2) Hagfeldt, A.; Gratzel, M. *Chem. Rev.* **1995**, *95*, 49.
 446 (3) Mills, A.; Lee, S. K. *J. Photochem. Photobiol., A* **2002**, *152*, 233.
 447 (4) Gopal, M.; Chan, W. J. M.; Jonghe, L. C. D. *J. Mater. Sci.* **1997**,
 448 *32*, 6001.
 449 (5) *Encyclopedia of Chemical Technology*; Mark, H. F., Othmer, D. F.,
 450 Overberger, C. G., Seaberg, G. T., Eds.; John Wiley: New York, 1983;
 451 Vol. 23, p 139.

(6) Weast, R. C. *Handbook of Chemistry and Physics*; CRC Press: 452
 Boca Raton, FL, 1984; p B-154.
 (7) Kostov, I. *Minerology*, 3rd ed.; Nauka, Izkustia, Sofia, 1973. 453
 (8) Yang, S. W.; Gao, L. *J. Am. Ceram. Soc.* **2005**, *88*, 968. 454
 (9) (a) Karakitsou, K. E.; Verykios, X. E. *J. Phys. Chem.* **1993**, *97*, 455
 1184. (b) McLoughlin, O. A.; Kehoe, S. C.; McGuigan, K. G.; Duffy, E. 456
 F.; Touati, F. A.; Gernjak, W.; Alberola, I. O.; Rodriguez, S. M.; Gill, L. 457
 W. *Solar Energy* **2004**, *77*, 657. 458
 (10) (a) Addamo, M.; Augugliaro, V.; Paola, D. A.; Lopez, G. E.; Loddò, 459
 V.; Marci, G.; Molinari, R.; Palmisano, L.; Schiavello, M. *J. Phys. Chem.* 460
B **2004**, *108*, 3303. (b) Lonnen, J.; Kilvington, S.; Kehoe, S. C.; Touati, F. 461
 A.; McGuigan, K. G. *Water Res.* **2005**, *39*, 877. 462
 (11) Hu, C.; Lan, Y.; Hu, X.; Wang, A. *J. Phys. Chem. B* **2006**, *110*, 463
 4066. 464
 (12) Sakatani, Y.; Grosso, D.; Nicole, L.; Boissiere, C.; Illia, S.; Sanchez, 465
 C. *J. Mater. Chem.* **2006**, *16*, 77. 466
 (13) Fujishima, A.; Rao, T. N.; Tryk, D. A. *J. Photochem. Photobiol.,* 467
C **2001**, *1*, 1. 468
 (14) Parkin, I. P.; Palgrave, R. G. *J. Mater. Chem.* **2005**, *15*, 1689. 469
 (15) Mills, A.; Lee, S. K. *J. Photochem. Photobiol., A* **2006**, *182*, 470
 181. 471
 (16) Zzanderna, A. W.; Rao, C. N. R.; Honig, J. M. *Trans. Faraday* 472
Soc. **1958**, *54*, 1069. 473
 (17) Yoganarasimhan, S. R.; Rao, C. N. R. *Trans. Faraday Soc.* **1962**, 474
58, 1579. 475
 (18) Kumar, S. R.; Pillai, S. C.; Hareesh, U. S.; Mukundan, P.; Warriar, 476
 K. G. *Mater. Lett.* **2000**, *43*, 286. 477
 (19) Reidy, D. J.; Holmes, J. D.; Morris, M. A. *J. Eur. Ceram. Soc.* 478
2006, *26*, 1527. 479
 (20) Navrotsky, A.; Kleppla, O. J. *J. Am. Ceram. Soc.* **1967**, *50*, 480
 626. 481
 (21) Machida, M.; Norimoto, W. K.; Kimura, T. *J. Am. Ceram. Soc.* 482
2005, *88*, 95. 483
 (22) Rao, C. N. R.; Turner, A.; Hanig, J. M. *J. Phys. Chem.* **1959**, *11*, 484
 173. 485
 (23) Ranjit, K. T.; Willner, I.; Bossmann, S. H.; Braun, A. M. *Environ.* 486
Sci. Technol. **2001**, *35*, 154. 487
 (24) Reidy, D. J.; Holmes, J. D.; Nagle, C.; Morris, M. A. *J. Mater.* 488
Chem. **2005**, *15*, 3494. 489
 (25) Kumar, K. N. P.; Kiezer, K.; Burggraaf, A. *J. Mater. Chem.* **1993**, 490
3, 141. 491
 (26) Baiju, K. V.; Sibin, C. P.; Rajesh, K.; Pillai, P. K.; Mukundan, P.; 492
 Warriar, K. G. K.; Wunderlich, W. *Mater. Chem. Phys.* **2005**, *90*, 123. 493
 (27) Suresh, C.; Biju, V.; Mukundan, P.; Warriar, K. G. K. *Polyhedron* 494
1998, *17*, 3131. 495
 (28) Khimich, N. N.; Venzel, B. I.; Drozdova, I. A.; Koptelova, L. A. 496
Russ. J. Appl. Chem. **2002**, *75*, 1108. 497
 (29) Cheng, P.; Qiu, J.; Gu, M.; Shangguan, W. *Mater. Lett.* **2004**, *58*, 498
 3751. 499
 (30) Yuan, J.; Chen, M.; Shi, J.; Shangguan, W. *Int. J. Hydrogen Energy* 500
2006, *31*, 1326. 501
 (31) Yin, S.; Ihara, K.; Aita, Y.; Komatsu, M.; Sato, T. *J. Photochem.* 502
Photobiol., A **2006**, *179*, 105. 503
 (32) Zheng, J. Y.; Pang, J. B.; Qiu, K. Y.; Wei, Y. *Microporous* 504
Mesoporous Mater. **2001**, *49*, 189. 505
 (33) Bakardjieva, S.; Subrt, J.; Stengl, V.; Dianez, M. J.; Dianez, M. J. 506
 S.; Sayagues, M. J. *Appl. Catal., B* **2005**, *58*, 193. 507
 (34) Yin, S.; Aita, Y.; Komatsu, M.; Sato, T. *J. Eur. Ceram. Soc.* **2006**, 508
26, 2735. 509
 (35) Sakthivel, S.; Janczarek, M.; Kisch, H. *J. Phys. Chem. B* **2004**, 510
108, 19384. 511
 (36) Yates, H. M.; Nolan, M. G.; Sheel, D. W.; Pemble, M. E. *J.* 512
Photochem. Photobiol., A **2006**, *179*, 213. 513
 (37) Yamamoto, Y.; Moribe, S.; Ikoma, T.; Akiyama, K.; Zhang, Q.; 514
 Saito, F.; Kubota, S. T. *Mol. Phys.* **2006**, *104*, 1733. 515
 (38) Spurr, R. A.; Myers, H. *Anal. Chem.* **1957**, *29*, 760. 516
 (39) Kung, H. H.; Ko, E. I. *Chem. Eng. J.* **1996**, *64*, 203. 517
 (40) Ren, L.; Huang, X.; Sun, F.; He, X. *Mater. Lett.* DOI: 10.1016/ 518
 j.matlet.2006.04.097. 519
 (41) Shi, Z. M.; Ye, X. Y.; Liang, K. M.; Gu, S. R.; Pan, F. *J. Mater.* 520
Sci. **2003**, *22*, 1255. 521
 (42) Irie, H.; Watanabe, Y.; Hashimoto, K. *J. Phys. Chem. B* **2003**, *107*, 522
 5483. 523
 (43) Cheng, X.; Lou, Y.; Samia, A. C. S.; Burda, C.; Gole, J. L. *Adv.* 524
Funt. Mater. **2005**, *15*, 41. 525
 (44) Pillai, S. C.; Kelly, J. M.; McCormack, D. E.; Ramesh, R. *J. Mater.* 526
Chem. **2004**, *14*, 1572. 527
 (45) Pillai, S. C.; Kelly, J. M.; McCormack, D. E.; O'Brien, P.; Ramesh, 528
 R. *J. Mater. Chem.* **2003**, *13*, 2586. 529
 (46) Pillai, S. C.; Kelly, J. M.; McCormack, D. E.; Ramesh, R. *Mater.* 530
Sci. Technol. **2004**, *20*, 964. 531
 (47) Bokhimi, X.; Morales, A.; Novaro, O.; López, T.; Chimal, O.; 532
 Asomoza, M.; Gómez, R. *Chem. Mater.* **1997**, *9*, 2616. 533
 534

- 535 (48) Pillai, S. C.; Boland, S. W.; Haile, S. M. *J. Am. Ceram. Soc.* **2004**,
536 87, 1388.
537 (49) Boland, S. W.; Pillai, S. C.; Yang, W. D.; Haile, S. M. *J. Mater.*
538 *Res.* **2004**, 19, 1492.
539 (50) Sibin, C. P.; Kumar, S. R.; Mukundan, P.; Warriar, K. G. K. *Chem.*
540 *Mater.* **2002**, 14, 2876.
541 (51) (a) Abe, R.; Sayama, K.; Domen, K.; Arakawa, H. *Chem. Phys.*
542 *Lett.* **2001**, 344, 339. (b) Carp, O.; Huisman, C. L.; Reller, A. *Prog. Solid*
543 *State Chem.* **2004**, 32, 33.
- (52) Gandhe, A. R.; Naik, S. P.; Fernandes, J. B. *Microporous Mesopo-* 544
rous Mater. **2005**, 87, 103. 545
- (53) Hoffmann, M. R.; Martin, S. T.; Choi, W.; Bahnemann, D. W. 546
Chem. Rev. **1995**, 95, 69. 547
- (54) Acosta, D. R.; Martinez, A. I.; Lopez, A. A.; Magana, C. R. *J.* 548
Mol. Catal. A: Chem. **2005**, 228, 183. 549
- (55) Baiju, K. V.; Periyat, P.; Pillai, P. K.; Mukundan, P.; Warriar, K. 550
G. K.; Wunderlich, W. *Mater. Lett.* DOI: 10.1016/j.matlet.2006.07.124. 551